Letter

Magnetization reversal of a ferromagnetic Pt/Co/Pt film by helicity dependent absorption of visible to near-infrared laser pulses

Kihiro T. Yamada[1,2,*,†] Carl S. Davies[1,3,*,‡] Fuyuki Ando,[4] Tian Li,[4] Teruo Ono[4,5,6] Theo Rasing,[1] Alexey V. Kimel,[1] and Andrei Kirilyuk[1,3]

[1]*Radboud University, Institute for Molecules and Materials, Nijmegen 6525 AJ, The Netherlands*
[2]*Department of Physics, Institute of Science Tokyo, Tokyo 152-8551, Japan*
[3]*FELIX Laboratory, Radboud University, Toernooiveld 7, Nijmegen 6525 ED, The Netherlands*
[4]*Institute for Chemical Research, Kyoto University, Uji 611-0011, Japan*
[5]*Center for Spintronics Research Network, Institute for Chemical Research, Kyoto University, Uji, 611-0011, Japan*
[6]*Center for Spintronics Research Network (CSRN), Graduate School of Engineering Science, Osaka University, Toyonaka 560-8531, Japan*

(Received 4 January 2022; accepted 24 December 2024; published 15 January 2025)

The practical difficulty in distinguishing the impact of magnetic circular dichroism and the inverse Faraday effect fuels intense debates over which mechanism predominantly drives the process of helicity dependent all-optical switching of magnetization in ferromagnets. Here, we quantitatively measure the efficiency of the switching process in a Pt/Co/Pt multilayer stack using visible- to near-infrared optical pulses. We find that the switching efficiency increases by a factor of 8.6 upon increasing the pumping wavelength from 0.5 to 1.1 μm, becoming 100% efficient at even longer wavelengths up to 2.0 μm. Our experimental results can be successfully explained by the phenomenon of magnetic circular dichroism, making a significant step towards resolving the long-standing controversy over the origin of the all-optical process of magnetization reversal in ferromagnets.

DOI: 10.1103/PhysRevB.111.L020406

The discovery of demagnetization on a subpicosecond timescale by a femtosecond (fs) laser pulse gave birth to the research field of ultrafast magnetism [1]. Furthermore, the use of circularly polarized pulses allows magnetization dynamics to be selectively excited according to the optical helicity [2–4]. Helicity-dependent control of magnetization precession was demonstrated in the dielectric $DyFeO_3$ by Kimel *et al.* [2], which was attributed to the inverse Faraday effect (IFE) [3]. Subsequently, similar effects have also been observed in magnetic semiconductors [4] and metals [5,6]. For some magnetic metals, magnetization can be switched by fs circularly polarized laser pulses in the absence of an external magnetic field. This phenomenon is referred to as all-optical helicity-dependent switching (AO-HDS). AO-HDS was demonstrated in ferrimagnetic GdFeCo [7] and later in ferromagnetic metals, including multilayered Co/Pt [8–15] and Co/Ni [8,10] stacks and granular FePt [16,17]. All-optical magnetization switching in GdFeCo films is driven by fast and efficient heating of electrons by the fs laser pulse [18] that brings the ferrimagnetic medium to a strongly nonequilibrium state [19]. The helicity dependence of the switching is derived from magnetic circular dichroism (MCD), which leads to different laser absorption levels that depend on the helicity [20], but the switching, in general, relies only on the fast heating. In ferromagnetic metals, in contrast, it is evident that circularly polarized pulses are genuinely indispensable for AO-HDS. However, when discussing the dominant mechanism that causes the switching in such systems, one always encounters the outstanding question: Do nonthermal or thermal effects drive the AO-HDS?

On the one hand, the IFE is well known to be nondissipative [3,21]. A circularly polarized fs pulse induces a magnetization in magnetic media via impulsive stimulated Raman processes [22], which is not accompanied by absorbing photons. Microscopic three-temperature models [23] and an atomistic spin model [24] all show that the magnetic polarity of a ferromagnetic metal can indeed be switched by the IFE.

On the other hand, the absorption of a fs laser pulse by a magnetic metal quasi-instantaneously elevates the metal's temperature on a nonequilibrium timescale, resulting in ultrafast demagnetization [1]. Because the optical absorption of a ferromagnetic metal varies according to the helicity via the MCD, helicity dependent laser absorption may be relevant to AO-HDS [24,25]. When magnetic domains of opposite polarity are illuminated by a circularly polarized pulse, their free energies decrease depending on the combination of optical helicity and magnetic orientation. As a result of repeating this process, magnetic domains with lower free energies should expand and eventually form a single magnetic domain, the final orientation of which depends on the helicity of the circularly polarized pulse.

Through testing how the pulse width [11] and starting temperature [13] affect AO-HDS in Pt/Co/Pt heterostructures, previous works have suggested that the MCD effect

*These authors contributed equally.
†Contact author: yamada@phys.sci.isct.ac.jp
‡Contact author: c.davies@science.ru.nl

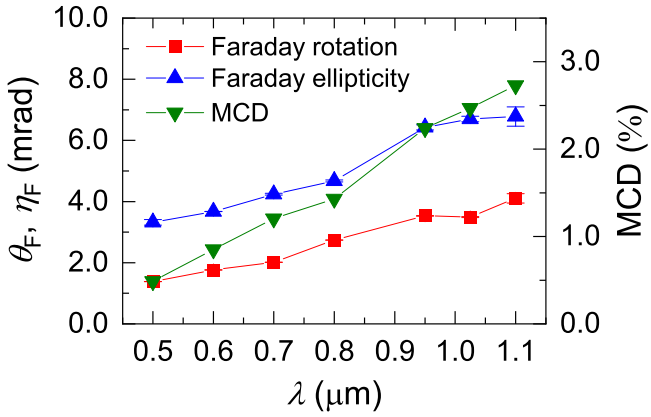

FIG. 1. The experimentally measured spectral dependencies of Faraday rotation θ_F, Faraday ellipticity η_F, and magnetic circular dichroism MCD of the studied Pt/Co/Pt multilayered stack.

drives the AO-HDS. For the case of AOS of magnetization in ferrimagnetic GdFeCo alloys, its spectral dependence was used to exclude the possible contribution of the IFE [20]. Investigating the spectral dependence of AO-HDS could similarly resolve the dominant driving mechanism of AO-HDS in Pt/Co/Pt multilayer stacks.

In this Letter, we investigate multipulse AO-HDS of a ferromagnetic Pt/Co/Pt system from the visible to near-infrared spectral ranges to elucidate whether AO-HDS is dominated by thermal or nonthermal effects. We experimentally find that the switching efficiency—defined as the amount of magnetization that is selectively switched by circularly polarized light—is enhanced by a factor of 8.6 upon increasing the optical wavelength from 0.5 to 1.2 μm. A phenomenological model of the inverse Faraday effect cannot explain this improved switching efficiency. Instead, we find that the effective magnetic field originating from the helicity dependent laser absorption increases by a factor of 32 in this spectral range, convincingly demonstrating that our results can be quantitatively described as a consequence of MCD.

Perpendicularly magnetized Pt/Co/Pt structures represent the most standard systems for studies of AO-HDS of ferromagnets [8–15]. We therefore used similar materials, depositing Ta (1.0 nm)/MgO (2.0 nm)/Pt (3.0 nm)/Co (0.6 nm)/Pt (3.0 nm)/Ta (4.0 nm) on a synthetic glass substrate by magnetron sputtering. We summarize in Fig. 1 the Faraday rotation θ_F and ellipticity η_F of the Pt/Co/Pt stack in the range of wavelengths λ between 0.5 and 1.2 μm, measured using a monochromator in combination with a photoelastic modulator [26]. Figure 1 shows that θ_F and η_F increase, within this spectral range, by factors of ∼3.0 and ∼2.0 respectively. We also determined the magneto-optical parts of the refractive indices of the Co and Pt layers using a transfer matrix method (see Ref. [27] and Supplemental Material Note 1 [28] for details of this method). We thus calculate the MCD defined as MCD $= (A^- - A^+)/[(1/2)\,(A^+ + A^-)]$, where $A^{+(-)}$ is the total absorption of right (left) circularly polarized light by the up-magnetized film. The spectral dependence of MCD is also plotted in Fig. 1, showing that MCD increases by a factor of ∼4.2 with increasing λ in the considered spectral range.

To excite the Pt/Co/Pt system, we used optical pulses ($\lambda = 800$ nm) delivered by an amplified Ti:Sa laser system at a repetition rate of 1 kHz. For $\lambda = 800$ nm, the pulse width was characterized using an autocorrelator to be 60 fs. By pumping an optical parametric amplifier (OPA), the central wavelength can be adjusted in the range $\lambda = 0.5$–2.0 μm. To obtain circular polarization across this broad spectral range, we used suitable quarter-wave plates AQWP05M-600 and AQWP05M-980 (Thorlabs Inc.) for $\lambda = 0.5$–0.8 and 0.95–1.1 μm, respectively, and PO-TWP-L4-25-IR (ALPHALAS GmbH) for $\lambda = 1.2$–2.0 μm. We found the ellipticity of the pump laser pulse induced by these achromatic quarter-wave plates, at each wavelength, to be consistently larger than 0.9. The train of circularly polarized optical pulses was focused on the surface of the uniformly magnetized Pt/Co/Pt sample. We characterized the Gaussian spot size on the sample at each wavelength by Liu's method [20,29]. The incident fluence was determined by using the extracted spot size and the laser power measured in front of the sample. To evaluate the switching efficiency of AO-HDS, we perform sweeping experiments whereby the sample is mounted on a motorized stage, enabling the laser pulses to be swept 100 μm across the sample at a constant speed of 10 μm/s. We used the magneto-optical Faraday effect to directly visualize the magnetization after exposure to the multiple optical pulses. Linearly polarized white light illuminates the sample and is collected by a ×20 objective lens. Depending on whether the magnetization of the sample is parallel or antiparallel to the wave vector of the transmitted light, the latter's polarization rotates in different senses. An analyzer, therefore, enables an image of magnetization to be detected using a charge-coupled-device camera.

Figure 2(a) displays typical snapshots recorded after sweeping the Pt/Co/Pt sample with pulses at $\lambda = 0.5$, 0.8, 1.1, and 2.0 μm for the four cases $(M^{\uparrow}, \sigma^+)$, $(M^{\uparrow}, \sigma^-)$, $(M^{\downarrow}, \sigma^+)$, and $(M^{\downarrow}, \sigma^c)$, respectively. Here, we use the notation $(M^{\uparrow\downarrow}, \sigma^{\pm})$ to indicate that the sample had initial magnetization pointing up $M^{\uparrow}$ or down $M^{\downarrow}$ and the impinging optical pulses were circularly polarized with right-handed σ^+ or left-handed σ^- helicity. Here, the electric field vectors of σ^+ and σ^- light projected on a screen rotate clockwise and anticlockwise, respectively, when standing against the light source. Figure 2(a) clearly shows that AO-HDS appears to become more efficient with increasing λ. To quantify the spectral dependence of the AO-HDS, we estimate the net switched magnetization $\langle M \rangle$ as follows. First, we averaged the intensities in a central rectangular area spanning 80 μm × 20 μm (364 × 91 pixels) on the track of the laser spot, as shown in Fig. 2(a). Second, $\langle M \rangle$ was estimated by normalizing the average with a reference image recorded for the sample in a uniformly magnetized state. Figure 2(b) shows $\langle M \rangle$ as a function of the laser incident fluence F for $\lambda = 0.5$, 0.8, 1.1, and 2.0 μm. The helicity dependence of the switching becomes increasingly stronger with increasing λ. In particular, the helicity dependence emerges when the fluence exceeds the demagnetization threshold (Fig. S2 [28]), where switched domains start to appear at the center of the spot because the laser fluence is high enough to excite the magnetization beyond the Curie temperature. As previously reported [8], AO-HDS demands heating of the system close to the Curie temperature. Figure 3(a) plots the

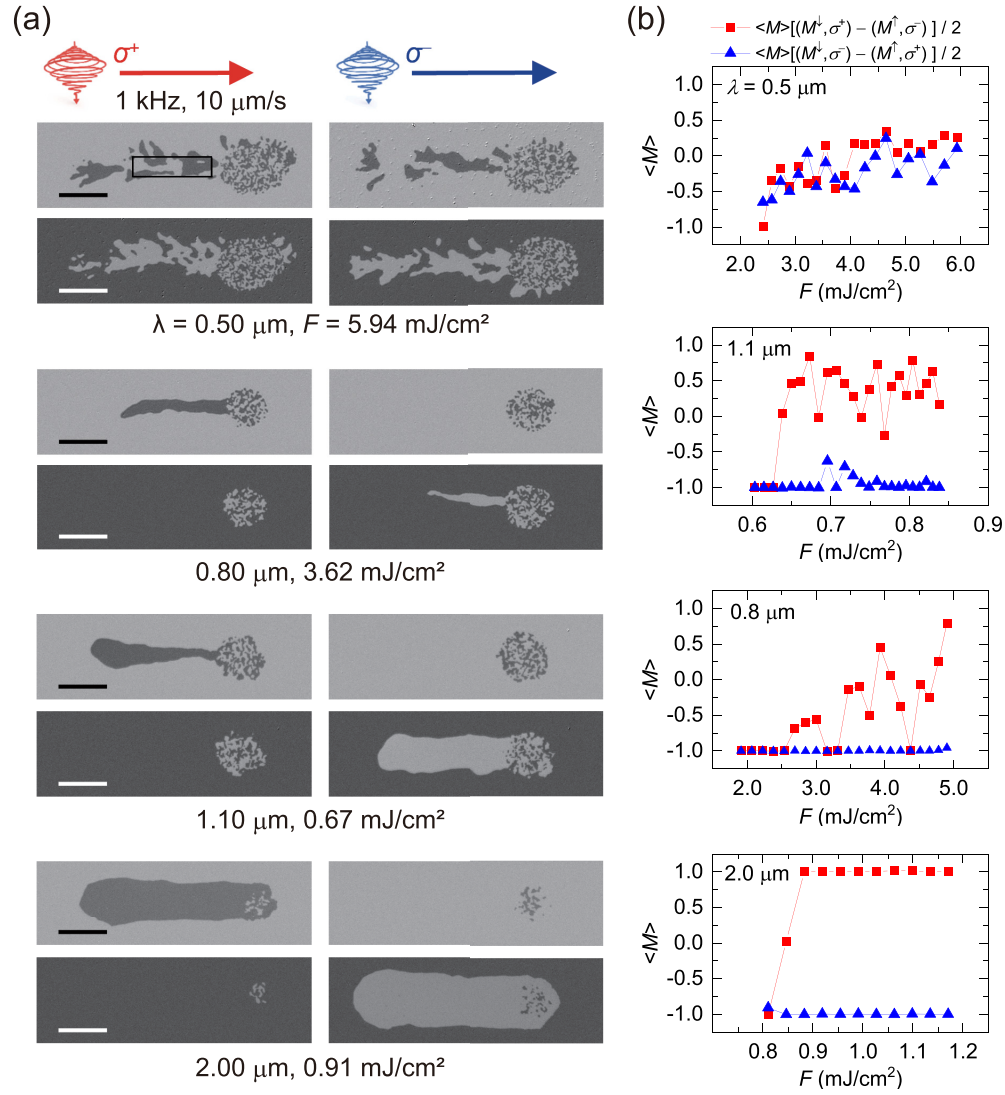

FIG. 2. (a) Typical results of multipulse all-optical helicity dependent switching (AO-HDS) for pumping wavelengths λ of 0.5, 0.8, 1.1, and 2.0 μm as indicated. Dark and bright contrasts correspond to up- and down-magnetized domains (pointing into or out of the plane of the page), respectively. Incident optical fluences (F) are shown below the snapshots. The scale bars correspond to 30 μm. We integrated the intensity in the rectangle of 20 μm × 80 μm to evaluate the net magnetization $\langle M \rangle$. (b) $\langle M \rangle$ as a function of F for $\lambda = 0.5$, 0.8, 1.1, and 2.0 μm. The red (blue) points correspond to the case when the spin angular momentum of light is antiparallel (parallel) to the magnetization direction of the original state.

extracted switching efficiency as $\varepsilon = \langle M \rangle\,[(M^{\uparrow}, \sigma^{+}) - (M^{\uparrow}, \sigma^{-}) + (M^{\downarrow}, \sigma^{+}) - (M^{\downarrow}, \sigma^{-})]/4$ versus λ, where we average the net magnetization $\langle M \rangle$ obtained for all fluences larger than that defining the demagnetization threshold. The spectral dependence of ε represents our key experimental finding and will be used later for quantitatively discussing which mechanism—the IFE or the MCD effect—principally drives the AO-HDS. The switching efficiency ε increases by a factor of ∼8.6 from $\lambda = 0.5$ μm to $\lambda = 1.1$ μm; ε reaches 100% (i.e., full switching) when $\lambda \geqslant 1.2$ μm. Simultaneously, we find that the minimum incident optical fluence required for AO-HDS decreases quite substantially as λ increases, that is, the process becomes more energy efficient for longer wavelengths [see Fig. 2(b)].

The pulse width is known to have a significant influence on AO-HDS. Extending the pulse durations to several picoseconds when optically irradiating multilayered $[Pt/Co]_3$ stacks, for example, significantly promotes the switching efficiency compared to using 60-fs pulses [11]. It is therefore important to assess the pulse durations delivered across the broad range of wavelengths supplied by the OPA. In lieu of suitably broadband standard detection methods, we indirectly assessed the pulse width of the OPA output using single-shot all-optical switching in GdFeCo [30,31] (see Supplemental Material Note 3 [28]). Figure S4 shows that the pulse width is nearly constant at ∼100 fs for all wavelengths tested, except for an anomaly around 0.55–0.75 μm where it rises to 200–350 fs. While our employed method for measuring the pulse duration is not as precise as standard techniques (such as frequency-resolved optical gating [32]), the obtained results plausibly show that the observed variation of ε cannot be explained by an elongation of the pulse width with increasing λ.

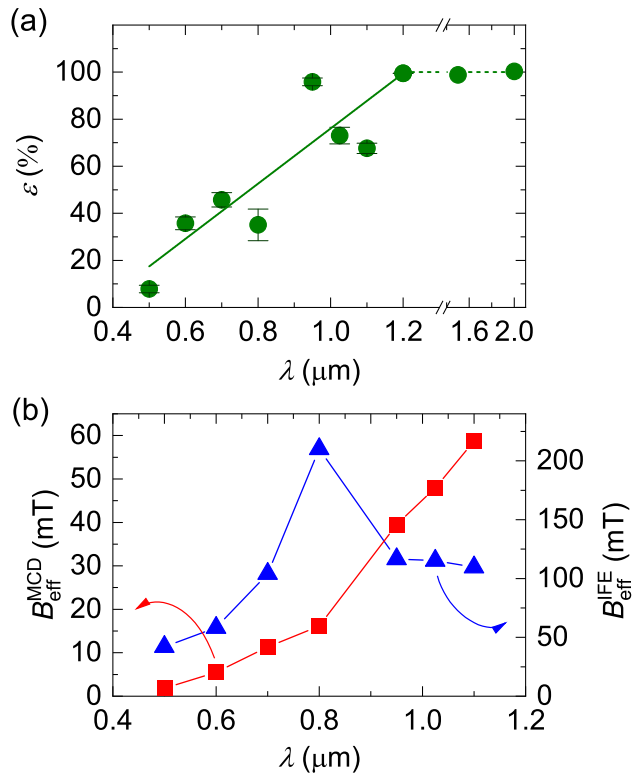

FIG. 3. (a) The spectral dependence of the switching efficiency ε, obtained by averaging the efficiencies measured for varying incident fluences above the threshold of demagnetization. The solid line is a linear fit for points between $\lambda = 0.5$ and 1.1 μm. (b) The spectral dependencies of the effective fields B_{eff} associated with the inverse Faraday effect (blue triangles) and the MCD effect (red squares).

We first evaluate the spectral dependence of AO-HDS originating from the helicity dependent laser absorption via MCD. In general, this model [9,11,14] explains AO-HDS in terms of a two-step process. In the first step, the thermal load delivered by an optical pulse induces demagnetization in the central area of the Gaussian spot, creating many domain walls (DWs) within a multidomain state. In the second step, subsequent circularly polarized optical pulses drive DW motion. The direction of the latter is defined by the MCD, since the circularly polarized optical pulse is preferentially absorbed by one of the magnetic domains compared to the other. Because the "hotter" domain has smaller free energy than the cooler domain, the DW moves opposite to the direction of the heat current [11]. Thus, the temperature gradient induced by the difference in optical absorption (originating from MCD) leads to DW motion that ultimately switches the net magnetization.

To model this process, a DW excited by a circularly polarized pulse experiences an effective magnetic field $B_{\text{eff}}^{\text{MCD}}$ created by a one-dimensional thermal gradient $\partial T/\partial x$ through the MCD [33]:

$$B_{\text{eff}}^{\text{MCD}} = -\frac{2}{Ml}\frac{\partial A}{\partial T}\frac{\partial T}{\partial x}, \tag{1}$$

where M, A, and l denote the saturation magnetization, exchange stiffness, and domain-wall width, respectively. Assuming that the irradiated region is heated from room temperature ($T_0 = 300$ K) towards the Curie temperature ($T_C = 470$ K) [34], the one-dimensional thermal gradient acting across the DW is $\partial T/\partial x = \text{MCD}\ (T_C - T_0)/l$. Note that the thermal gradient is on the order of 0.01–0.1 K/nm, which is four orders of magnitude larger than that required to move the DW of a magnetic garnet [35]. Using the temperature dependencies of M, A, and l given in Ref. [36], we estimate the $B_{\text{eff}}^{\text{MCD}}$ from $M(T) = M(0)[1-(T/T_C)^{2.37}]^{0.34}$, $A(T) = A(0)[M(T)/M(0)]^{1.82}$, $l(T) = l(0)[M(T)/M(0)]^{-0.59}$. We also simply assume the temperature dependence of the MCD as $\text{MCD}(T) = \text{MCD}(0)[M(T)/M(0)]$. The values at $T = 0$ K are estimated by using $M(300) = 1.13 \times 10^6$ A/m, $A(300) = 1.6 \times 10^{-11}$ J/m, and $l(300) = 6.6$ nm following Ref. [34]. The results are plotted in Fig. 3(b) and show a monotonic increase of $B_{\text{eff}}^{\text{MCD}}$ with wavelength, similar to the experimentally observed increase of the efficiency in that spectral range [Fig. 3(a)].

We next estimate the $B_{\text{eff}}^{\text{IFE}}$ produced by the IFE using a phenomenological approach [21]. The IFE induces a magnetization along the direction given by the cross product of the light's electrical field and its complex conjugation, $\mathbf{E} \times \mathbf{E}^*$. The resultant magnetization, which is qualitatively equivalent to an effective magnetic field, is therefore nominally capable of switching the magnetization direction. In an isotropic magnetic medium, the strength of the effective magnetic field of the IFE [21] is given by

$$B_{\text{eff}}^{\text{IFE}} = \frac{\theta_F \lambda n F}{\pi M c \tau d}, \tag{2}$$

where c, τ, d, and F denote the speed of light, the pulse width, the stack thickness, and the optical fluence, respectively. For the estimation, we fixed the pulse width at 60 fs for all wavelengths and used the thickness-weighted average of the real parts of the refractive indices of the Co and Pt layers [28]. Here, we considered the sum of the fluences, at the threshold of demagnetization, between an optical pulse propagating downward from the MgO/Pt interface and one propagating upward from the Pt/Ta interface. Although the handedness of a circularly polarized pulse changes by reflection, the IFE of the reflected pulse has the same sign as that of the incident pulse because of the inversion of the k vector. Figure 3(b) indicates that the calculated effective magnetic field induced by the IFE has a rather different spectral dependence. Although the $B_{\text{eff}}^{\text{IFE}}$ also initially rises, it has a clear maximum at $\lambda = 0.8$ μm, whereafter it decreases to almost half from the maximum at $\lambda = 1.1$ μm. This is in stark contrast with the clear experimental observation of ε scaling monotonically with increasing λ [Fig. 3(a)].

In the spectral range 0.5–1.1 μm, the switching efficiency ε increases monotonically by a factor of ~8.6 [Fig. 3(a)]. In the same spectral range, the $B_{\text{eff}}^{\text{MCD}}$ also increases monotonically (by a factor of ~32) while the spectral dependence of $B_{\text{eff}}^{\text{IFE}}$ does not accord with that of ε [Fig. 3(b)]. Thus, the dramatic improvement of the AO-HDS with increasing λ can quantitatively be explained by the spectral dependence of the MCD effect but not by that of the IFE. Therefore, we conclude that the MCD effect predominantly drives the AO-HDS.

To ensure that our conclusion is not limited to a single Pt/Co/Pt stack, we also investigated the spectral dependence

of AO-HDS found in a Pt (3 nm)/Co (0.8 nm)/Pt (3 nm) multilayer using the same procedures (see Supplemental Material Note 4 [28]). We observed a similar monotonic improvement of AO-HDS with increasing λ for this thicker multilayer, which is explained by the monotonically increasing MCD effect. Moreover, we studied the AO-HDS in a [Pt (2 nm)/Co (0.8 nm)]$_2$/Pt (2 nm) heterostructure. Again, for the multilayer with different lamination, we observed a similar enhancement of AO-HDS with increasing λ (see Supplemental Material Note 4 [28]). These results, obtained for different nanolayer-thicknesses and laminations, indicate the robustness of our conclusion—namely, that the MCD effect dominates AO-HDS for ferromagnets in the visible to near-infrared spectral ranges.

Note that the duration of B_{eff} is also important for magnetization switching. On the one hand, the impulsive stimulated Raman process associated with the IFE is only active while the optical pulse is present in the system, and so the duration of $B_{\mathrm{eff}}^{\mathrm{IFE}}$ is equivalent to the duration of the employed fs pulse. On the other hand, the duration of $B_{\mathrm{eff}}^{\mathrm{MCD}}$ will be much longer, because the isothermalization of two immediately adjacent magnetic domains will proceed across timescales on the order of hundreds of picoseconds or more. Therefore, although the peak amplitude of the $B_{\mathrm{eff}}^{\mathrm{MCD}}$ is smaller, the temporal integration of its effect will be much larger than that obtained from $B_{\mathrm{eff}}^{\mathrm{IFE}}$.

We also note the limitation of the phenomenological model of the inverse Faraday effect: the Faraday rotation does not necessarily agree with the inverse Faraday effect for absorbing magnetic media [37]. *Ab initio* calculations may be useful to more accurately discuss the contribution of the IFE to the AO-HDS. It is anticipated from Eq. (2) and the *ab initio* calculations from Ref. [38] that $B_{\mathrm{eff}}^{\mathrm{IFE}}$ diverges for increasing λ and a constant fluence. Investigating AO-HDS with infrared pulses in a free-electron laser facility [39,40] is a future work planned to gain more insight into the possibility of using IFE to achieve AO-HDS. Although we have tested three different Pt/Co/Pt multilayered stacks, AO-HDS is observed also in other thin ferromagnetic [8,10] as well as ferrimagnetic [41,42] metals. We anticipate that a similar methodological study of a much larger class of materials could ultimately lead to an even better generalized understanding of AO-HDS. In particular, a sign inversion of the Kerr ellipticity close to $\lambda = 500$ nm was recently reported in a sperimagnetic alloy of TbCo [26]. Assuming that MCD drives the switching, pumping this sample at wavelengths above and below this threshold would presumably reverse the symmetry of AO-HDS.

To summarize, we have investigated the spectral dependence of AO-HDS in a Pt/Co/Pt multilayered stack, in the visible to the near-infrared spectral regime, to ascertain the dominant mechanism that drives the process. We have experimentally found that the multipulse AO-HDS effect becomes increasingly efficient upon increasing the excitation wavelength, reaching 100% at wavelengths greater than 1.2 μm. The monotonic enhancement of the switching efficiency follows that of the effective field associated with the helicity dependent laser absorption (MCD), while the inverse Faraday effect cannot explain the improved AO-HDS. Our results provide crucial and experimentally grounded insight into the origin of AO-HDS in ferromagnetic metals.

The authors thank S. Semin and C. Berkhout for technical support, and A. Tsukamoto for providing the GdFeCo sample. This research has received funding from de Nederlandse Organisatie voor Wetenschappelijk Onderzoek (NWO) and the European Union's Horizon 2020 research and innovation program under FET Open Grant Agreements No. 713481 (SPICE) and No. 737093 (FEMTOTERABYTE) and ERC Grant Agreement No. 856538 (3D-MAGiC). This work was partially supported also by JSPS KAKENHI Grants No. 22K14588, No. 24K00938, No. 15H05702, No. 20K22327, No.20H00332, No. 20H05665, No. 17J07326, and No. 18J22219, by the Collaborative Research Program of the Institute for Chemical Research, Kyoto University, and by the Spintronics Research Network of Japan (Spin-RNJ).

[1] E. Beaurepaire, J.-C. Merle, A. Daunois, and J.-Y. Bigot, Ultrafast spin dynamics in ferromagnetic nickel, Phys. Rev. Lett. **76**, 4250 (1996).

[2] A. V. Kimel, A. Kirilyuk, P. A. Usachev, R. V. Pisarev, A. M. Balbashov, and Th. Rasing, Ultrafast non-thermal control of magnetization by instantaneous photomagnetic pulses, Nature (London) **435**, 655 (2005).

[3] P. S. Pershan, J. P. van der Ziel, and L. D. Malmstrom, Theoretical discussion of the inverse Faraday effect, Raman scattering, and related phenomena, Phys. Rev. **143**, 574 (1966).

[4] P. Němec, E. Rozkotová, N. Tesařová, F. Trojánek, E. De Ranieri, K. Olejník, J. Zemen, V. Novák, M. Cukr, P. Malý, and T. Jungwirth, Experimental observation of the optical spin transfer torque, Nat. Phys. **8**, 411 (2012).

[5] C. D. Stanciu, F. Hansteen, A. V. Kimel, A. Tsukamoto, A. Itoh, A. Kirilyuk, and Th. Rasing, Ultrafast interaction of the angular momentum of photons with spins in the metallic amorphous alloy GdFeCo, Phys. Rev. Lett. **98**, 207401 (2007).

[6] G.-M. Choi, A. Schleife, and D. G. Cahill, Optical-helicity-driven magnetization dynamics in metallic ferromagnets, Nat. Commun. **8**, 15085 (2017).

[7] C. D. Stanciu, F. Hansteen, A. V. Kimel, A. Kirilyuk, A. Tsukamoto, A. Itoh, and Th. Rasing, All-optical magnetic recording with circularly polarized light, Phys. Rev. Lett. **99**, 047601 (2007).

[8] C.-H. Lambert, S. Mangin, B. S. D. Ch. S. Varaprasad, Y. K. Takahashi, M. Hehn, M. Cinchetti, G. Malinowski, K. Hono, Y. Fainman, M. Aeschlimann, and E. E. Fullerton, All-optical control of ferromagnetic thin films and nanostructures, Science **345**, 1337 (2014).

[9] M. S. El Hadri, P. Pirro, C.-H. Lambert, S. Petit-Watelot, Y. Quessab, M. Hehn, F. Montaigne, G. Malinowski, and S. Mangin, Two types of all-optical magnetization switching

mechanisms using femtosecond laser pulses, Phys. Rev. B **94**, 064412 (2016).

[10] M. S. El Hadri, M. Hehn, P. Pirro, C.-H. Lambert, G. Malinowski, E. E. Fullerton, and S. Mangin, Domain size criterion for the observation of all-optical helicity-dependent switching in magnetic thin films, Phys. Rev. B **94**, 064419 (2016).

[11] R. Medapalli, D. Afanasiev, D. K. Kim, Y. Quessab, S. Manna, S. A. Montoya, A. Kirilyuk, Th. Rasing, A. V. Kimel, and E. E. Fullerton, Multiscale dynamics of helicity-dependent all-optical magnetization reversal in ferromagnetic Co/Pt multilayers, Phys. Rev. B **96**, 224421 (2017).

[12] Y. Quessab, R. Medapalli, M. S. El Hadri, M. Hehn, G. Malinowski, E. E. Fullerton, and S. Mangin, Helicity-dependent all-optical domain wall motion in ferromagnetic thin films, Phys. Rev. B **97**, 054419 (2018).

[13] U. K. Parlak, R. Adam, D. E. Bürgler, S. Gang, and C. M. Schneider, Optically induced magnetization reversal in $[Co/Pt]_N$ multilayers: Role of domain wall dynamics, Phys. Rev. B **98**, 214443 (2018).

[14] G. Kichin, M. Hehn, J. Gorchon, G. Malinowski, J. Hohlfeld, and S. Mangin, From multiple- to single-pulse all-optical helicity-dependent switching in ferromagnetic Co /Pt multilayers, Phys. Rev. Appl. **12**, 024019 (2019).

[15] F. Cheng, Z. Du, X. Wang, Z. Cai, L. Li, C. Wang, A. Benabbas, P. Champion, N. Sun, L. Pan, and Y. Liu, All-optical helicity-dependent switching in hybrid metal-ferromagnetic thin films, Adv. Opt. Mater. **8**, 2000379 (2020).

[16] Y. K. Takahashi, R. Medapalli, S. Kasai, J. Wang, K. Ishioka, S. H. Wee, O. Hellwig, K. Hono, and E. E. Fullerton, Accumulative magnetic switching of ultrahigh-density recording media by circularly polarized light, Phys. Rev. Appl. **6**, 054004 (2016).

[17] R. John, M. Berritta, D. Hinzke, C. Müller, T. Santos, H. Ulrichs, P. Nieves, J. Walowski, R. Mondal, O. Chubykalo-Fesenko, J. McCord, P. M. Oppeneer, U. Nowak, and M. Münzenberg, Magnetisation switching of FePt nanoparticle recording medium by femtosecond laser pulses, Sci. Rep. **7**, 4114 (2017).

[18] T. A. Ostler, J. Barker, R. F. L. Evans, R. W. Chantrell, U. Atxitia, O. Chubykalo-Fesenko, S. El Moussaoui, L. Le Guyader, E. Mengotti, L. J. Heyderman, F. Nolting, A. Tsukamoto, A. Itoh, D. Afanasiev, B. A. Ivanov, A. M. Kalashnikova, K. Vahaplar, J. Mentink, A. Kirilyuk, Th. Rasing, and A. V. Kimel, Ultrafast heating as a sufficient stimulus for magnetization reversal in a ferrimagnet, Nat. Commun. **3**, 666 (2012).

[19] K. Vahaplar, A. M. Kalashnikova, A. V. Kimel, D. Hinzke, U. Nowak, R. Chantrell, A. Tsukamoto, A. Itoh, A. Kirilyuk, and Th. Rasing, Ultrafast path for optical magnetization reversal via a strongly nonequilibrium state, Phys. Rev. Lett. **103**, 117201 (2009).

[20] A. R. Khorsand, M. Savoini, A. Kirilyuk, A. V. Kimel, A. Tsukamoto, A. Itoh, and Th. Rasing, Role of magnetic circular dichroism in all-optical magnetic recording, Phys. Rev. Lett. **108**, 127205 (2012).

[21] A. Kirilyuk, A. V. Kimel, and Th. Rasing, Ultrafast optical manipulation of magnetic order, Rev. Mod. Phys. **82**, 2731 (2010).

[22] V. N. Gridnev, Phenomenological theory for coherent magnon generation through impulsive stimulated Raman scattering, Phys. Rev. B **77**, 094426 (2008).

[23] T. D. Cornelissen, R. Cordoba, and B. Koopmans, Microscopic model for all optical switching in ferromagnets, Appl. Phys. Lett. **108**, 142405 (2016).

[24] M. O. A. Ellis, E. E. Fullerton, and R. W. Chantrell, All-optical switching in granular ferromagnets caused by magnetic circular dichroism, Sci. Rep. **6**, 30522 (2016).

[25] J. Gorchon, Y. Yang, and J. Bokor, Model for multi-shot all-thermal all-optical switching in ferromagnets, Phys. Rev. B **94**, 020409(R) (2016).

[26] K. Satoh, Measurement of magneto-optical kerr effect using piezo-birefringent modulator, Jpn. J. Appl. Phys. **20**, 2403 (1981).

[27] C. C. Katsidis and D. I. Siapkas, General transfer-matrix method for optical multilayer systems with coherent, partially coherent, and incoherent interference, Appl. Opt. **41**, 3978 (2002).

[28] See Supplemental Material at http://link.aps.org/supplemental/10.1103/PhysRevB.111.L020406 for the estimation of magneto-optical coefficients of magnetic multilayer using a transfer-matrix formalism, the assessment of demagnetization threshold and the wavelength-dependent pulse duration, and the spectral dependence of AO-HDS for other Pt/Co/Pt multilayers, which includes Refs. [43–48].

[29] J. M. Liu, Simple technique for measurements of pulsed Gaussian-beam spot sizes, Opt. Lett. **7**, 196 (1982).

[30] C. S. Davies, T. Janssen, J. H. Mentink, A. Tsukamoto, A. V. Kimel, A. F. G. van der Meer, A. Stupakiewicz, and A. Kirilyuk, Pathways for single-shot all-optical switching of magnetization in ferrimagnets, Phys. Rev. Appl. **13**, 024064 (2020).

[31] C. S. Davies, G. Bonfiglio, K. Rode, J. Besbas, C. Banerjee, P. Stamenov, J. M. D. Coey, A. V. Kimel, and A. Kirilyuk, Exchange-driven all-optical magnetic switching in compensated 3*d* ferrimagnets, Phys. Rev. Res. **2**, 032044(R) (2020).

[32] R. Trebino, K. W. DeLong, D. N. Fittinghoff, J. N. Sweetser, M. A. Krumbügel, and D. J. Kane, Measuring ultrashort laser pulses in the time-frequency domain using frequency-resolved optical gating, Rev. Sci. Instrum **68**, 3277 (1997).

[33] F. Schlickeiser, U. Ritzmann, D. Hinzke, and U. Nowak, Role of entropy in domain wall motion in thermal gradients, Phys. Rev. Lett. **113**, 097201 (2014).

[34] P. J. Metaxas, J. P. Jamet, A. Mougin, M. Cormier, J. Ferré, V. Baltz, B. Rodmacq, B. Dieny, and R. L. Stamps, Creep and flow regimes of magnetic domain-wall motion in ultrathin Pt/Co/Pt films with perpendicular anisotropy, Phys. Rev. Lett. **99**, 217208 (2007).

[35] W. Jiang, P. Upadhyaya, Y. Fan, J. Zhao, M. Wang, L.-T. Chang, M. Lang, K. L. Wong, M. Lewis, Y.-T. Lin, J. Tang, S. Cherepov, X. Zhou, Y. Tserkovnyak, R. N. Schwartz, and K. L. Wang, Direct imaging of thermally driven domain wall motion in magnetic insulators, Phys. Rev. Lett. **110**, 177202 (2013).

[36] R. Moreno, R. F. L. Evans, S. Khmelevskyi, M. C. Muñoz, R. W. Chantrell, and O. Chubykalo-Fesenko, Temperature-dependent exchange stiffness and domain wall width in Co, Phys. Rev. B **94**, 104433 (2016).

[37] H. Watanabe and A. Daido, Generalized Pitaevskii relation between rectifying and linear responses: Application to

reciprocal magnetization induction, Phys. Rev. B **110**, 014405 (2024).

[38] M. Berritta, R. Mondal, K. Carva, and P. M. Oppeneer, *Ab Initio* theory of coherent laser-induced magnetization in metals, Phys. Rev. Lett. **117**, 137203 (2016).

[39] D. Oepts, A. F. G. van der Meer, and P. W. van Amersfoort, The free-electron-laser user facility FELIX, Infrared Phys. Technol. **36**, 297 (1995).

[40] G. M. H. Knippels, and A. F. G. van der Meer, F. E. L. diagnostics, and user control, Nucl. Instrum. Methods Phys. Res. **144**, 32 (1998).

[41] S. Mangin, M. Gottwald, C-H. Lambert, D. Steil, V. Uhlíř, L. Pang, M. Hehn, S. Alebrand, M. Cinchetti, G. Malinowski, Y. Fainman, M. Aeschlimann, and E. E. Fullerton, Engineered materials for all-optical helicity-dependent magnetic switching, Nat. Mater. **11**, 286 (2014).

[42] Y. Quessab, M. Deb, J. Gorchon, M. Hehn, G. Malinowski, and S. Mangin, Resolving the role of magnetic circular dichroism in multishot helicity-dependent all-optical switching, Phys. Rev. B **100**, 024425 (2019).

[43] K. H. Clemens and J. Jaumann, Magnetooptisehe und optisehe eigensehaften yon ferromagnetischen sehichten im ultraroten, Z. Phys. **173**, 135 (1963).

[44] J. H. Weaver, Optical properties of Rh, Pd, Ir, and Pt, Phys. Rev. B **11**, 1416 (1975).

[45] J. H. Weaver, D. W. Lynch, and C. G. Olson, Optical properties of V, Ta, and Mo from 0.1 to 35 eV, Phys. Rev. B **10**, 501 (1974).

[46] R. E. Stephens and I. H. Malitson, Index of refraction of magnesium oxide, J. Res. Natl. Bur. Stand. **49**, 249 (1952).

[47] T. J. Bright, J. I. Watjen, Z. M. Zhang, C. Muratore, A. A. Voevodin, D. I. Koukis, D. B. Tanner, and D. J. Arenas, Infrared optical properties of amorphous and nanocrystalline Ta_2O_5 thin films, J. Appl. Phys **114**, 083515 (2013).

[48] I. H. Malitson, Interspecimen comparison of the refractive index of fused silica, J. Opt. Soc. Am. **55**, 1205 (1965).